Nanoscale

www.rsc.org/nanoscale

Volume 2 | Number 1 | January 2010 | Pages 1–156

ISSN 2040-3364

RSC Publishing

COVER ARTICLE
Graham et al.
Mixed metal nanoparticle assembly
and the effect on surface-enhanced
Raman scattering

REVIEW
Lin et al.
Progress of nanocrystalline growth
kinetics based on oriented attachment

2040-3364(2010)2:1;1-T

Journal Name

ARTICLE TYPE

Highly sensitive free radical detection by nitrone-functionalized gold nanoparticles

Libo Du,[a] Saipeng Huang,[a] Qianfen Zhuang,[a] Hongying Jia,[a] Antal Rockenbauer,[d] Yangping Liu,*[b] Ke Jian Liu*[c] and Yang Liu*[a]
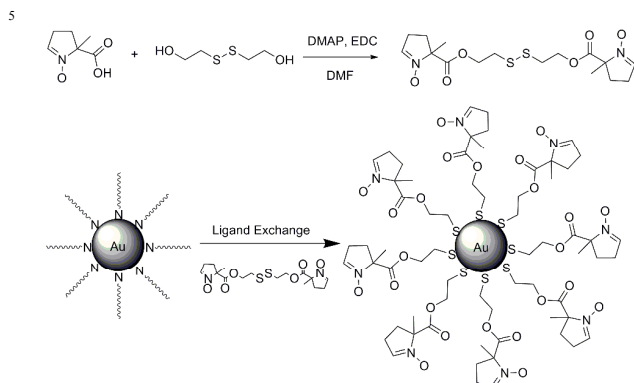
The detection of free radicals and related species has attracted signifcant attention in recent years because of their critical roles in physiological and pathological process. Among the methods for the detection of free radicals, electron spin resonance (ESR) coupled with the use of the spin trapping technique has been
10 an effective approach for characterization and quantification of these species due to their high specificity. However, its application in biological systems, especially in *in vivo* systems, has been greatly limited partially due to the low reaction rate between the currently available spin traps with biological radicals. To overcome this drawback, we herein report the first example of nitrone functionalized gold nanoparticles (Au@EMPO) as highly efficient spin trap in which the thiolated EMPO (2-
15 (ethoxycarbonyl)-2-methyl-3, 4-dihydro-2H-pyrrole 1-oxide) derivative was self-assemblied on gold nanoparticles. Kinetic studies showed that Au@EMPO has a 137-fold higher reaction rate constant with ˙OH than PBN (N-*tert*-butyl-alpha-phenylnitrone). Owing to the high rate of trapping ˙OH by Au@EMPO as well as high stability of the resulting spin adduct ($t_{1/2} \sim 56$min), Au@EMPO affords 124-fold higher sensitivity for ˙OH than EMPO. Thus, this new nano spin trap shows great potential in
20 trapping the important radicals such as ˙OH in various biological systems and provides a novel strategy to design spin traps with much improved properties.

Introduction

Free radicals play a key role in physiological and pathological processes including aging, cancer development, and
25 neurodegenerative diseases.[1-2]. To understand the biological role of free radicals, it is of critical importance to develop highly sensitive techniques for detection and quantitation of free radicals being produced. Although a number of methods such as fluorescent and HPLC methods[3-4] have been developed to detect
30 and identify free radicals, they are often limited by low specificity and sensitivity.[5] Compared with other approaches, electron spin resonance (ESR)-spin trapping technique, owing to its relative higher specificity, is believed to be an indispensable method for the detection of free radicals in biological systems.[6-8]
35 However, it has been demonstrated that high concentrations of spin traps (e.g., 50-100 mM) are often required to reach the detectable ESR signal because the currently available spin traps have much lower rate constants with biological radicals than endogenous antioxidants[9,10], which may induce potential
40 cytotoxicity. To overcome this limitation, a lot of effort has been devoted to develop nitrone spin traps with improved free radical traping rate and enhanced stability of the resulting spin adducts in the past decades.[11-12] However, low trapping efficiency remains a major problem.
45 Previous studies showed that self-assembled monolayer of

organic molecules on nanoparticles exhibits higher reactivity than the sum of the corresponding monomers possibly due to the high specific surface area of gold nanoparticles (AuNPs). For example, the reaction rate constant of azide with alkyne can be
50 significantly enhanced by self-assembly of the azide or alkyne on the surface of AuNPs.[13] Our recent studies also demonstrated that the rate constants of the antioxidants 6-hydroxy-2,5,7,8-tetramethylchroman-2-carboxylic acid or salvianolic acid A with free radicals can be enhanced by self-assembly of these
55 antioxidants on the surface of AuNPs.[14-15] We therefore hypothesize that the self-assembly of nitrone compounds on AuNPs can also increase their reactivity with free radicals. To test the hypothesis, we synthesized the AuNP-based nitrone spin trap Au@EMPO by ligand exchange of tetraoctylammonium
60 bromide-stabilized AuNPs with (EMPO-S)$_2$ (Scheme 1) which belongs to the derivative of 2-(ethoxycarbonyl)-2-methyl-3, 4-dihydro-2H-pyrrole 1-oxide (EMPO), a commonly used spin trap for hydroxyl radical (˙OH) and superoxide radical (O$_2$˙⁻). To our knowledge, this is the first example of nitrone-functionalized
65 AuNPs. We characterized the newly synthsized Au@EMPO by ultraviolet-visible absorption spectroscopy (UV-Vis, Fig. 1), Fourier transform infrared spectroscopy (FT-IR, Fig. S1), transmission electron microscopy (TEM), X-ray photoelectron spectrum (XPS) (Fig. 2), thermal gravimetric analysis (TGA, Fig.
70 S2), and inductively coupled plasma mass spectrometry (ICP-MS, Table S2). The reactivity of Au@EMPO towards ˙OH and

carbon-centered radicals were compared with N-*tert*-butyl-α-phenylnitrone (PBN) and EMPO using competitive kinetics. Moreover, spin trapping of $O_2^{\bullet-}$ by Au@EMPO was also investigated.

5

Scheme 1. Synthetic route of nitrone-functionalized gold nanoparticle (Au@EMPO).
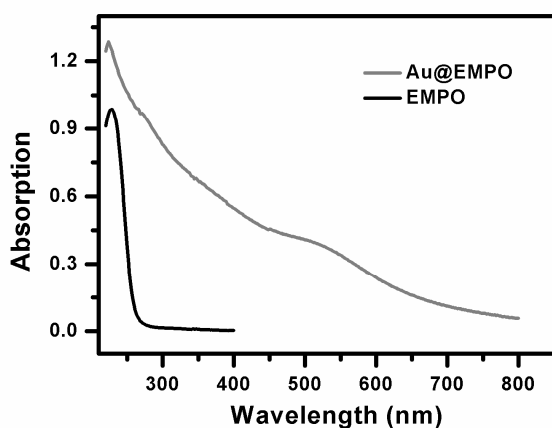

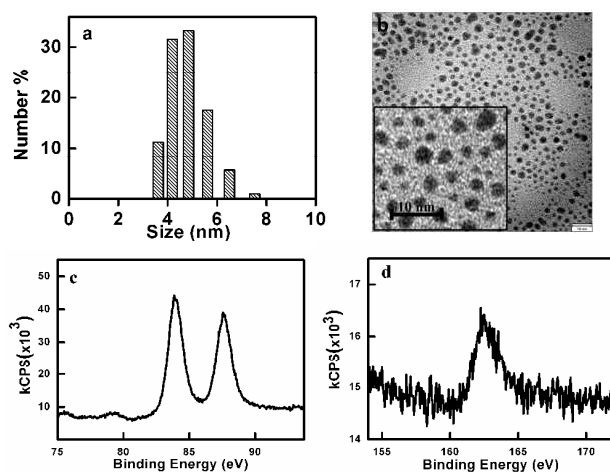**Fig. 1.** UV-Vis spectra of Au@EMPO and EMPO

10

Fig. 2. (a) Nanoparticle size distribution measured by dynamic light scattering (DLS); (b) TEM image of Au@EMPO; (c) XPS spectrum of Au4f7/2 and Au4f5/2;
15 (d) XPS spectrum of S2p3/2.

Results and discussion

Synthesis and characterization of self-assembled nano nitrones (Au@EMPO)

20 Scheme 1 shows the synthetic procedure of Au@EMPO. (EMPO-S)$_2$ was firstly obtained by conjugation of 5-carboxy-5-methyl-1-pyrroline N-oxide (CMPO)[16] with 2,2'-disulfanediyldiethanol using 1-ethyl-3-(3-dimethylaminopropyl) carbodiimide (EDCI) in the presence of 4-dimethylaminopyridine (DMAP) and 25 triethylamine (TEA). Subsequent ligand exchange of tetraoctylammonium bromide-stabilized AuNPs [17-18] with (EMPO-S)$_2$ in dichloromethane afforded Au@EMPO which was purified by Sephadex LH-20 column chromatography using dichloromethane : methanol (v/v =20:1) as an eluent. Unless 30 specified otherwise, the concentration of Au@EMPO used in this study refers to the molar concentration of EMPO (See the calculation method in the supporting information).

UV-Vis studies showed that Au@EMPO has both surface plasmon resonance (SPR) band of the AuNPs at ~520 nm and 35 absorption band of the EMPO moiety at ~239 nm (Fig. 1), verifying the self-assembly of (EMPO-S)$_2$ on the nanoparticles. This self-assembly behavior was further confirmed by the FT-IR spectrum of Au@EMPO (Fig. S1), in which an intensive peak between 1471 cm^{-1} and 1580 cm^{-1} assigned to the C=N stretching 40 vibration in thiolated-EMPO was observed. The absence of the S-H stretching mode in the FT-IR spectrum of Au@EMPO indicates the formation of the thiolate-gold bond between (EMPO-S)$_2$ and gold surface[19] and the covalent attachment of (EMPO-S)$_2$ on the surface of AuNPs. Furthermore, XPS study 45 showed that through the ligand exchange a significant proportion of the outer gold atoms in Au@EMPO was oxidized from Au^0 to Au^1 as observed by the oxidation shift of Au 4f7/2 peak from 83.8 eV to 84.4 eV (Fig. 2c), as well as S2p3/2 peak at 162.5 ev (Fig. 2d), further confirming the formation of the sulfur-gold 50 chemical bond.[20] TEM image shows that the average diameter of the nanoparticle core in the Au@EMPO is 4.5 nm (Fig. 2a). Based on the results of TEM, XPS (Fig. 2, Table S1), TGA (Fig. S2) and ICP-MS (Table S2), the representative chemical formula of Au@EMPO can be defined as Au$_{1441}$@EMPO$_{592}$.[15]

55

Fig. 3. *In vitro* stability studies of Au@EMPO by monitoring UV-vis absorption peak at ~535 nm wavelength, (a) 1h; (b) 15 days.

In vitro stability and biocompatibility study

60 In order to test if Au@EMPO is suitable for *in vivo* applications, its stability was evaluated by monitoring the plasmon wavelength (λmax) and plasmon bandwidth (Δλ) in phosphate buffer solutions (pH 5.5-8.5), 10% NaCl and 0.5% bovine serum albumin (BSA), or in Dulbecco's modified eagle 65 medium containing 10% fetal bovine serum. The plasmon wavelengths of the nanoparticles in all the above solutions

showed minimal shifts (< 5nm) over the period of a half month, indicating that Au@EMPO has excellent stability under different conditions and is suitable for long-term storage (Fig. 3). These results suggest that the Au@EMPO has good stability for *in vivo* 5 applications. Moreover, water solubility of Au@EMPO was found to be as high as 20 mg mL^{-1}, (the concentration of Au, data not shown) which is significantly higher than that of AuNPs used *in vitro* and *in vivo*.[21-22] On the other hand, no hemolysis of red blood cells (RBCs) in the presence of Au@EMPO was detected 10 at the concentrations of up to 100 μg cm^{-3} (the concentration of Au), as shown in Table S3 of Supporting Information.

Moreover, we used $SO_3^{\bullet-}$ adduct as our model system to examine the stability of the adducts with Au@EMPO and spin trap monomers according to the method described in the previous 15 study.[23] Briefly, the *in vitro* stability of the spin adducts was examined by rapidly mixing preformed spin adducts with ascorbate in room air, and following the decay rate of the spin adducts. The decay of the adduct follows approximately first order kinetics. In the absence of ascorbate, the lifetime of 20 Au@EMPO/$SO_3^{\bullet-}$ and EMPO/$SO_3^{\bullet-}$ was 216 and 51 min, respectively, while in the presence of 2 mM ascorbate, the lifetime was 52 and 8.3 min, respectively. In both cases, Au@EMPO/$SO_3^{\bullet-}$ is significantly more stable than EMPO/$SO_3^{\bullet-}$. The reducing/oxidizing abilities of Au@EMPO and EMPO were 25 also measured by cyclic voltammetry. The results showed that the reducing potential of the spin adduct of Au@EMPO was much lower than that of EMPO (data not shown), indicating that the spin adduct of EMPO is more easily reduced than Au@EMPO. Therefore, it could be concluded that the nanoparticle-spin trap is 30 more stable than that of spin trap monomer.These results showed that Au@EMPO has great stability and biocompatibility for potential *in vivo* biological applications.
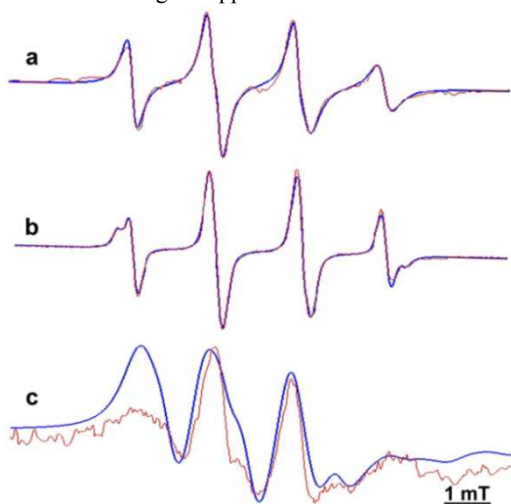

Fig. 4. Experimental (orange) and simulated (blue) ESR spectra of (a) Au@EMPO-
35 OH (A$_N$ = 1.39 mT and A$_H$ = 1.23 mT). Au@EMPO (27 μM) was incubated with the Fenton system consisting of H_2O_2 (2 mM), EDTA (2 mM), Fe^{2+} (2 mM). (b) EMPO-OH (A$_N$ = 1.41 mT and A$_H$ = 1.29 mT for the major component and A$_N$ = 1.46 mT and A$_H$ = 1.61 mT for the minor component); the same as (a) but in the presence of EMPO (10 mM) instead of Au@EMPO. (c) Au@EMPO-OOH (g$_{zz}$ =
40 2.0021, g$_{xx}$ = g$_{yy}$ = 2.0102, A$_{Nzz}$= 3.25mT, A$_{Nxx}$ = A$_{Nyy}$ = 0.67 mT, A$_{Hzz}$ = 1.18 mT, A$_{Hxx}$ = A$_{Hyy}$ = 0.94 mT, τ= 17.6 ns). Au@EMPO (27 μM) were mixed with 18-crown-6 (160 mM) and KO_2 (10 mM) in DMSO.

Spin trapping of hydroxyl radical by Au@EMPO and stability of the corresponding spin adduct

45 To demonstrate the high sensitive spin trapping properties of the newly designed nano spin trap Au@EMPO, spin trapping of $^{\bullet}$OH generated by the Fenton system was used as an example. As shown in Fig. 4a, while Au@EMPO-hydroxyl spin adduct was observable using an extremely low concentration of Au@EMPO 50 (27 μM), same concentration of EMPO did not produce any detectable signal. In fact, an EMPO concentration of 10 mM was required to obtain a signal to achieve a similar ESR signal intensity of Au@EMPO-OH, which suggests that Au@EMPO has much higher efficiency to trap $^{\bullet}$OH than EMPO. The ESR 55 spectrum of Au@EMPO-hydroxyl spin adduct consists of a four lines due to the similar hyperfine splitting constants (A$_N$=1.39 mT and A$_H$ = 1.23mT) from the nitrogen (*I*=1) and β-hydrogen (*I*=1/2) nuclei. Interestingly, this ESR spectrum exhibits distinct anisotropy as evidenced by the broader and
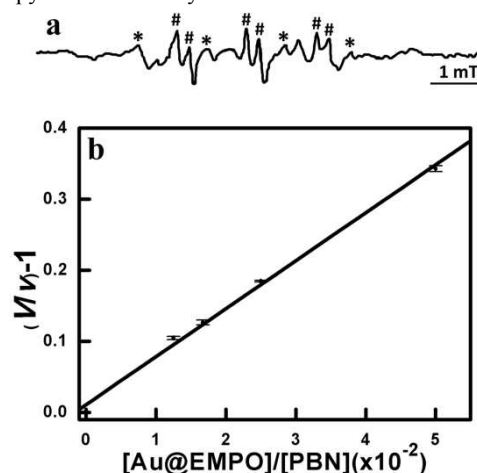

60 **Fig. 5.** (a) The representative ESR spectrum of the mixture of Au@EMPO-OH and PBN/•OH which were generated from the UV photolysis of H_2O_2 in the presence of both Au@EMPO and PBN, #, Au@EMPO-OH; *, PBN-OH; (b) typical plot of V/v-1 vs [Au@EMPO]/[PBN] using the competitive experiments. The solution 65 containing H_2O_2 (0.33 mM), PBN (10 mM), DTPA (0.1 mM) and various concentrations of Au@EMPO (0, 13, 17, 25 and 50 μM) in PBS (0.1 M, pH 7.4) was irradiated by UV irradiation (254 nm). The growth of the ESR signal of Au@EMPO-OH was monitored for 3 min upon the irradiation and the initial rate of the Au@EMPO-OH formation was obtained.

70 weaker high-field line than that of the EMPO adduct, possibly due to slower molecular tumbling (Fig. 4a). In order to compare the correlation time of tumbling, we carried out computer simulation of the ESR spectra by extending our former automatic 75 fitting program [24] by introducing a slow motion model, where exchange jumps are integrated over all characteristic orientations. The method is based on the fact that even for isotropic spectra the line width variation in the hyperfine patterns depends on the anisotropy of g- and hyperfine tensors and changes 80 characteristically as a function of correlation time. The line shape function for the jumps can be obtained from the modified Bloch equations developed for conformational exchanges between two sites. The procedure can reproduce well the line shapes for the cases of slow, intermediate or fast tumbling. Fig. 4c shows an 85 example for the intermediate line shape close to the rigid powder

pattern. In the automatic fitting procedure, the two axial principal values of g, A_N and A_H tensors were optimized together with the rotational correlation time (τ). The calculations showed that Au@EMPO-OH has an estimated τ of 0.561 ns compared to τ =0.080 ns for EMPO-OH. The principal values of tensors were essentially the same for the two radical adducts: g_{zz}=2.0026, g_{xx}=g_{yy}=2.0089, A_{Nzz}=3.01mT, A_{Nxx}=A_{Nyy}=0.6 mT, A_{Hzz}=1.72 mT, A_{Hxx}=A_{Hyy}=1.01 mT. The high τ value for Au@EMPO-OH could be attributed to the immobilization of its spin adduct moiety on the surface of AuNPs. This result is consistent with the previous observation that the τ value of spin label immobilized on the hybrid nanoparticles was much longer than that of free forms due to the mobility decrease of the spin label.[25] It was also shown that the high-field peaks of the spin adduct of the PBN functionalized polymer (polyPBN) were considerably broader than those of the corresponding monomer due to the restricted motion of the nitroxide moiety in the polymer.[26] These
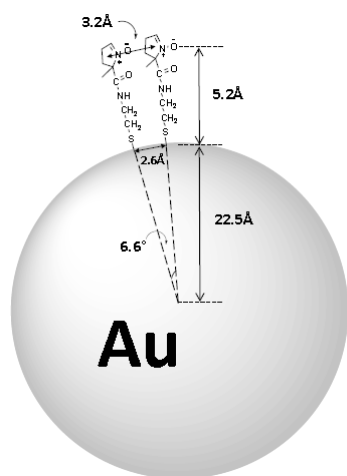

Fig. 6. Schematic illustration of Au@EMPO. Assuming that the gold nanoparticle core is an ideal sphere, the average distance between two ligands in Au@EMPO can be estimated to be 3.2 Å according to the size (4.5 nm) of the nanoparticle core, the number (n = 592) of the ligands on each nanoparticle and the linker distance (5.2 Å).

results support our notion that the broader and weaker high field line of Au@EMPO-OH was induced by the decreased mobility of the Au@EMPO-OH adduct. To provide further evidence, the $^{\bullet}$OH generating system using UV photolysis of H_2O_2 was utilized to investigate decay kinetics of the hydroxyl spin adduct of Au@EMPO. As shown in Fig. S3, the ESR signal of Au@EMPO-OH persisted for as long as 180 min with the half-life time of $t_{1/2}$=56 min, which was much longer than that of EMPO-OH ($t_{1/2}$=36 min). The higher stability of Au@EMPO-OH than EMPO-OH is most likely due to slow molecular mobility and/or steric protection induced by the AuNPs.

The spin trapping kinetic study of Au@EMPO

As mentioned above, Au@EMPO at the very low concentration (i.e., 27 µM) was able to afford a detectable EPR signal of its hydroxyl spin adduct possibly because of the high stability of this adduct (Fig. S3) and the high trapping rate. In order to quantitatively evaluate the trapping efficiency of Au@EMPO and elucidate the nano effect on its spin trapping properties, the

second-order rate constant for the reaction between Au@EMPO and $^{\bullet}$OH (Equation 1) was measured by competition with PBN and compared with that of EMPO. Fig. 5a shows the representative ESR spectrum obtained by incubation of both Au@EMPO and PBN with the $^{\bullet}$OH-generating system. The well separated ESR signal of Au@EMPO-OH from that of PBN/$^{\bullet}$OH allows for monitoring the formation kinetics of Au@EMPO-OH in the presence of various concentrations of Au@EMPO. The data are plotted using Equation 1 where V and v are the initial rates of $^{\bullet}$OH adducts formation (i.e. the slope of the linear-fitted equation) in the absence and presence of Au@EMPO, respectively. Similarly, the reaction rate constant of EMPO with $^{\bullet}$OH was also measured. Results showed that the rate constant for Au@EMPO with •OH was 137 times greater than PBN (Fig. S4). In contrast, the rate constant of EMPO with $^{\bullet}$OH was just 1.1 times higher than that of PBN. Based on the reported reaction rate constant of PBN with $^{\bullet}$OH(k_{PBN} = $6.1 \times 10^9 M^{-1}$ s^{-1}),[27-28] $k_{Au@EMPO}$ was calculated to be 8.35×10^{11} M^{-1} s^{-1} which is 124-fold higher than k_{EMPO} (6.71×10^9 M^{-1} s^{-1}). Similar nano effect on the spin trapping rate was also observed in the experiments of trapping α–hydroxyethyl radical ($^{\bullet}$CH(CH$_3$)OH) in aqueous solution (Fig. S5, S6) with a 174-fold higher reaction rate constant for Au@EMPO vs EMPO. From the above calculation, it is interesting to note that the second order rate constant for the reaction of Au@EMPO and $^{\bullet}$OH was greater than the diffusion rate constant $10^9 \sim 10^{10}$ M^{-1} s^{-1}. To our knowledge, it is impossible for the second order rate constant to be higher than the diffusion rate constant. The reason for this result, we speculated, can be attributed to the competitive calculation methods we used, which relies only on the concentration of the spin traps (as shown in Equation 1). As mentioned above, Au@EMPO at the very low concentration (i.e., 27 µM) was able to afford the detectable EPR signal of its hydroxyl spin adduct. In contrast, EMPO at the same concentration (27 µM) could not generate any signal, and required a much higher concentration (e.g., 10 mM) to obtain a signal with the similar ESR signal intensity of Au@EMPO-OH. Therefore, based on the Equation 1, the second order rate constant for the reaction between the nano-particlized Au@EMPO and $^{\bullet}$OH would be much greater than that of the non-nano-particlized PBN or EMPO. Although we still yet need to fully understand how a second order rate constant for nano-particles could be greater than diffusion controlled rate, the results from the calculation illustrates that Au@EMPO has a more sensitive detection capacity on the free radicals than spin trap monomers.

$$\frac{V}{v} - 1 = \frac{K_{Au@EMPO}[Au@EMPO]}{K_{PBN}[PBN]} \quad [1]$$

The mechanism of enhanced free radical detection of Au@EMPO

Previous studies showed that the intermolecular H-bond between pyrrole-NH and nitronyl-O increase the positive charge of nitronyl-C and accordingly accelerate the reaction between the nitrones and $^{\bullet}$OH.[29-31] In our case, the relative short distance (~3.2 Å, Fig. 6) among two adjacent nitrone groups in Au@EMPO allows for the intermolecular interactions of the ligands, which

can be confirmed by the considerable red-shift of the maximum UV-vis absorption (239 nm) due to the nitronyl group in Au@EMPO as compared to that of EMPO monomer (232 nm, Fig. S7). Therefore, we speculated that the enhanced rate constant
5 for the reaction of Au@EMPO with free radicals may be due to the intermolecular interactions between two adjacent nitrone groups on the surface of Au@EMPO. If so, it can be expected that the reaction rate constant of Au@EMPO with ˙OH would be influenced by the intermolecular distance between the nitrone
10 groups on AuNPs. To test this hypothesis, a new EMPO coated gold nanoparticles (Au@PEG3) with a long thiolated triethylene glycol (PEG3) as linker was synthesized (see Scheme S1, Fig. S8-S10). Kinetic studies showed that as expected, Au@PEG3EMPO had a much lower rate constant for ˙OH
15 $(2.15 \times 10^{11} M^{-1} s^{-1})$ than Au@EMPO (Fig. S11-S12), supporting our hypothesis that the intermolecular interaction among the nitronyl groups on the surface of AuNPs is a key factor in determining the reaction rate constant of the nitrone with •OH. On the other hand, a previous study[26] illustrated that the spin-
20 trapping reactivity of the PBN functionalized polymer (polyPBN) was associated with the ratio of styrene-unit (St) and nitrone-unit (Nt). Specifically, the spin trapping reactivity of polyPBN increases as the ratio of Nt to St decreases. The authors suggested that the less steric hindrance accounted for the faster reaction
25 between free radical and polyPBN as the proportion of Nt to St decreases. In our opinion, it may be due to the distance decrease between the Nt's on the polymer as a result of the decrease of the amount of St. Therefore, we believe that such results gave further support to our hypothesis. Interestingly, the reaction rate of
30 Au@EMPO with •OH or •CH (CH₃)OH is much faster than the rate of the diffusion control, which needs further studies to understand more detailed mechanisms.

Spin trapping of superoxide anion by Au@EMPO

Since $O_2^{˙-}$ is considered as the primary upstream radical of the
35 radical reaction chain under the oxidative stress and has been implicated in many pathophysiological processes,[32] considerable attention has been paid to the detection of this radical in biological systems. In this study, Au@EMPO was used to trap $O_2^{˙-}$ that was generated by the KO₂/18-crown-6/DMSO system.
40 Owing to the high sensitivity of Au@EMPO for free radicals, a low concentration of Au@EMPO (27 μM) was used and the resulting ESR signal of the superoxide spin adduct exhibited an intensive anisotropy possibly due to dense packing of the spin adduct moiety on AuNPs (Fig. 3c) and the highly viscous DMSO
45 as a solvent. The computer simulation gave in this case a rather long correlatin time: τ = 17.6 ns. Although attempts to obtain rate constants of Au@EMPO with $O_2^{˙-}$ by competition with PBN were not successful due to the overlapping of their ESR signals, a detectable ESR signal of the adduct with such low concentration
50 of 27μM Au@EMPO as compared to 10mM of EMPO clearly demonstrates that Au@EMPO has a much higher rate constants with $O_2^{˙-}$ than EMPO.

Conclusion

In conclusion, we have demonstrated the first example of nitrone-
55 functionalized AuNPs (Au@EMPO) as a highly sensitive spin

trap for various free radicals. Meanwhile, the prepared Au@EMPO is remarkable stable in various buffer solutions. The Au@EMPO exhibit significantly enhanced spin trapping rate constants with ˙OH and ˙CH(CH₃)OH with 124 and 174 fold
60 higher rate constants, respectively, than EMPO. This nano effect on the spin trapping rate can be attributed to the intermolecular interactions among the adjacent nitrone groups induced by the self-assembly of the nitrone spin trap on AuNPs. These nano spin traps shows great application potential to detect and quantitate
65 free radicals in chemical, biochemical and biomedical systems and provides a brand new strategy to develop spin traps with enhanced reaction rates with free radicals.

Experimental

Synthesis of (EMPO-S)₂

70 To a solution of 2,2'-disulfanediyldiethanol (0.308g, 2mmol) [2] and CMPO (0.684g, 4mmol) in DMF (15mL) were added EDCI (1.488g, 9.6 mmol) and DMAP (1.171g, 9.6 mmol) with stirring at 0°C for 1h and then TEA was added (1.336 mL, 9.6 mmol). The resulting mixture was stirred overnight at room temperature.
75 Then, the mixture was evaporated and redissolved in CHCl₃ (100 mL). The resulting solution was washed with HCl (1N, 10 ml) and concentrated NaHCO₃ (20 mL), dried over Na₂SO₄ and concentrated in vacuo. Subsequent purification by flash chromatography (Petroleum ether:EtOAc=20:1, R_f=0.26)
80 afforded the pure product as a white solid (Yield: 51%). Liquid chromatography analysis showed that the purity of (EMPO-S)₂ was over 95%.¹H-NMR (400 MHz, D₂O): δ 0.99 (s, 6H), 1.80 (m, 4H), 3.02-3.06 (m, 8H), 3.10-3.13 (m, 4H), 7.31-7.35 (m, 2H). ¹³C-NMR (400 MHz, D₂O): δ 14.4, 25.0, 34.9, 36.4, 39.2, 55.3,
85 117.7, 160.6. (Figure S13, S14) HR MS (FAB) *m/z* calculated for C₁₆H₂₄N₂O₆S₂: 404.1076, measured: 404.1062.

Synthesis of Nitrone-Functionalized gold nanoparticles

An aqueous solution of hydrogen tetrachloroaurate (0.1 g, 0.29mM) and H₂O (1.9 ml) was mixed with tetraoctylammonium
90 bromide (0.5g, 0.92 mM) in toluene (14 ml). The two-phase mixture was vigorously stirred until all the tetrachloroaurate was transferred into the organic phase, which turned deep orange in color while the aqueous phase became colourless. Then, sodium borohydride (60mg, 1.58 mM) in 8ml of water was slowly added
95 to the above solution under stirring. Within a few seconds the organic phase changed from orange to ruby red. After further stirring for 20min, the organic phase was extracted, washed with distilled water (5 × 15 ml), dried with anhydrous Na₂SO₄ and then concentrated. The resulting residue was redissovled in
100 CH₂Cl₂ (5 ml), and then (EMPO-S)₂ was added. The resulting suspension was stirred under N₂ for 1 day. After removal of the solvent, the slurry of the crude Au@EMPO was redissolved in methanol (3 ml) and purified by Sephadex LH-20 column chromatography using dichloromethane: methanol (1:1) as eluent
105 to give the pure nanoparticles (Au@EMPO) as dry powder which was stored at -20°C until use. The ¹H-NMR spectrum of Au@EMPO can be observed in Fig. S15.

Kinetic Studies of $\cdot$OH Trapping

All kinetic experiments were performed in phosphate-buffered saline containing diethylenetriaminepentaacetic acid (DTPA, 0.1 mM) as an iron chelator. The hydroxyl radical ($\cdot$OH) was generated by UV photolysis of H_2O_2 (0.330 mM). All solutions were bubbled with nitrogen gas prior to irradiation. The sample cell was irradiated with a Spectroline low-pressure mercury vapor lamp with 0.64cm×5.4cm dimensions and a 254 nm wavelength. The second-order rate constants of Au@EMPO and EMPO with $\cdot$OH were determined using PBN as a competitor. While a constant concentration of PBN (10 mM) was used, the concentration of Au@EMPO or EMPO was varied from 0 to 50 µM for Au@EMPO or from 1.62 to 8.13 mM for EMPO. Incremental EPR spectra were recorded 30 s after irradiation for 3 min. The initial spin-trapping rate was determined within 120 s by monitoring the first low-field peak intensity of Au@EMPO-OH or EMPO-OH. All data were the average of three or more measurements.

In vitro stability studies

In vitro stability of the Au@EMPO was tested in the presence of NaCl, bovine serum albumin (BSA), Dulbecco's modified eagle medium, fetal bovine serum. Typically, 0.5 mL of Au@EMPO solution (20mg ml^{-1}) was added to glass vials containing 0.5 ml of NaCl (10%), 0.5% bovine serum albumin (BSA), pH 5.5, 7.4 and 8.5 phosphate buffer solutions, Dulbecco's modified eagle medium, 10% fetal bovine serum, respectively, and incubated for 30 min. We also have studied the *in vitro* stability with various phosphate buffers (pH 5.5, 7.4 and 8.5) following the similar procedure described above. The stability and identity of the Au@EMPO were measured by recording UV absorbance at 1 h as well as after 15 days after storing at room temperature. The surface plasmon resonance band at 530 nm confirmed the retention of nanoparticulates in all the above mixtures.

Acknowledgements

Notes and references

^{a} State Key Laboratory for Structural Chemistry of Unstable and Stable Species, Centre for Molecular Science, Institute of Chemistry, Chinese Academy of Sciences, Beijing, 100190, P.R. China. Fax: +86 10 62559373; Tel:+86 10 62571074; E-mail: yliu@iccas.ac.cn.
^{b} School of Pharmacy, Tianjin Medical University, Tianjin 300070, P. R. China. Email: ypliu@iccas.ac.cn
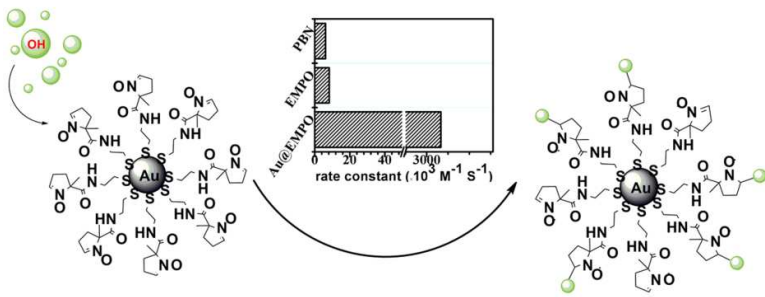*^{c} College of Pharmacy, University of New Mexico, Albuquerque, NM 87131, USA. Email: kliu@salud.unm.edu.*
^{d} Institute of Molecular Pharmacology, Research Center for Natural Sciences, H-1025 Budapest, Pusztaszeri 59, Hungary.
† Electronic Supplementary Information (ESI) available: [details of any supplementary information available should be included here]. See DOI: 10.1039/b000000x/

1   M. Valko, C. J. Rhodes, J. Moncol, M. Izakovic and M. Mazur, *Chem.-Biol. Interact.,* 2006, **160**, 1.
2   J. Schetter, N. H. Heegaard and C. C. Harris, *Carcinogenesis*, 2010, **31**, 37.
3   S. Reuter, S. C. Gupta and M. M. Chaturvedi, *Free Radic. Biol. Med.,* 2010, **49**, 1603.
4   G. M.Rosen, B. E.Britigan, H. J. Halpern and S.Pou, Free Radicals: Biology and Detection by Spin Trapping. OxfordUniversity Press, 1999.
5   K. Ranguelova, A. B. Rice, A. Khajo, M. Triquigneaux, S. Garantziotis, R. S. Magliozzo and R. P. Mason, *Free Radic. Biol. Med.,* 2012, **52**, 1264.
6   K. V. Darley-Usmar, K. J. A. Davies, P. A. Dennery, H. J. Forman, M. B. Grisham, G. E. Mann, K. Moore, L. J. Roberts II and H. Ischiropoulos, *Free Radic. Biol. Med.*, 2012, **52**, 1.
7   M. Hardy, A. Rockenbauer, J. Vásquez-Vivar, C. Felix, M. Lopez, S. Srinivasan, N. Avadhani, A. Tordo and B. Kalyanaraman, *Chem. Res. Toxicol.*, 2007, **20**, 1053.
8   M. Hardy, D. Bardelang, H. Karoui, A. Rockenbauer, J. P. Finet, L. Jicsinszky, R. Rosas, O. Ouari and P. Tordo, *Chem. Eur. J.*, 2009, **15**, 11114.
9   R. P. Mason, *Free. Radic. Biol. Med.* 2004, **36**, 1214.
10 S. Pou, D. J. Hassett, B. E. Britigan, M. S. Cohen and G. M. Rosen, *Anal. Biochem.*, 1989, **177**, 1.
11 S. U. Kim,Y. Liu, K. M. Nash, J. L. Zweier, A. Rockenbauer and F. A. Villamena, *J. Am. Chem. Soc.,* 2010, **132**, 17157; T. Oka, S.Yamashita, M. Midorikawa, S. Saiki, Y. Muroya, M. Kamibayashi, K. Yamashita, K. Anzai and Y. Katsumura, *Anal. Chem.* 2011, **83**, 9600.
12 M. Moreno, F. J. Ibanez, J. B. Jasinski and F. P. Zamborini, *J. Am. Chem. Soc.*, 2011, **133**, 4389.
13 J. Thode and M. E. Williams, *J. Colloid. Inter. Sci.,* 2008, **320**, 346.
14 Z. Nie, K. J. Liu, C. J. Zhang, L. F. Wang, Y. Yang, Q.Tian and Y. Liu, *Free. Radic. Biol. Med.,* 2007, **43**, 1243.
15 L. Du, S. Suo, G. Wang, H. Jia, K. J. Liu, B. Zhao and Y. Liu, *Chem. Eur. J.*, 2013, **19**, 1281.
16 P. Tsai, M. Elas, A. D. Parasca, E. D. Barth, C. Mailer, H. J. Halpern and G. M. Rosen, *J. Chem. Soc., Perkin Trans. 2*, 2001, 875.
17 J. Fink, C. J. Kiely, D. Bethell and D. Schiffrin, *J. Chem. Mater.*, 1998, **10**, 922.
18 A. Manna, P. L. Chen, H. Akiyama, T. X. Wei, K. Tamada and W. Knoll, *Chem. Mater.*, 2003, **15**, 20.
19 C. Templeton, M. P. Wuelfing and R. W. Murray, *Acc. Chem. Res.* 2000, **33**, 27.
20 H. Y. Jia, Y. Liu, X. J. Zhang, L. Han, L. B. Du, Q. Tian and Y. C. Xu, *J. Am. Chem. Soc.*, 2009, **131**, 40.
21 G. F. Paciotti, D. G. I. Kingston and L. Tamarkin, *Drug Develop. Res.*, 2006, **67**, 47.
22 M. E. Davis, J. E. Zuckerman, C. H. J. Choi, D. Seligson, A. Tolcher, C. A. Alabi, Y. Yen, J. D. Heidel and A. Ribas, *Nature,* 2010, **464**, 1067.
23 K. J. Liu, M. Miyake, T. Panz and H. Swarz, *Free. Radic. Biol. Med.* 1999, **26**, 714.
24 A. Rockenbauer and L. Korecz, *Appl. Magn. Reson.,* 1996, **10**, 29.
25 C. Ghica and P. Ionita, *J. Mater. Sci.,* 2007, **42**, 10058; V. K. Khlestkin, J. F. Polienko, M. A. Voinov, A. I. Smirnov and V. Chechik, *Langmuir,* 2008, **24**, 609; P. Ionita, A. Volkov, G. Jeschke and V. Chechik, *Anal. Chem.,* 2008, **80**, 95.
26 N. Kuno, K. Sakakibar, M. Hirota and T. Kogane, *React. Funct. Polym.,* 2000, **43**, 43.
27 R. Sridhar, P. C. Beaumont and E. L. Powers, *J. Radioanal. Nucl. Chem.*, 1986, **101**, 227.
28 L. Greenstock and R. H. Wiebe, *Can. J. Chem.,* 1982, **60**, 1560.
29 F. A. Villamena., C. M. Hadad and J. L. Zweier, *J. Phys. Chem. A.,* 2003, **107**, 4407.
30 R. A. Burgett., X. Bao and F. A. Villamena, *J. Phys. Chem. A* 2008, **112**, 2447.
31 S.-U. Kim., Y. Liu., K. M. Nash., J. L. Zweier, A. Rockenbauer and F. A. Villamena, *J. Am. Chem. Soc.,* 2010, **132**, 17157.
32 Halliwell and J. M. C. Gutteridge, Free Radicals in Biology and Medicine, 4 th ed.; Oxford University: New York, 2007.

TOC

We report the first example of nitrone functionalized gold nanoparticles as highly efficient spin trap for free radical detection.